Available online at www.sciencedirect.com
SCIENCE DIRECT®
PERGAMON
Mechanism and Machine Theory 38 (2003) 379–394
MECHANISM AND MACHINE THEORY
www.elsevier.com/locate/mechmt

On the kinematic constraint surfaces of general three-legged planar robot platforms

M.J.D. Hayes [a,*], M.L. Husty [b]

[a] *Department of Mechanical and Aerospace Engineering, Carleton University, 1125 Colonel By Drive, Ottawa, Ont., Canada K1S 5B6*

[b] *Institut für Technische Mathematik, Geometrie, und Bauinformatik, Universität Innsbruck, Technikerstrasse 13, A-6020 Innsbruck, Austria*

Received 2 March 2001; received in revised form 17 June 2002; accepted 20 August 2002

Abstract

The variants of general three-legged planar robot platforms are enumerated and classified. Constraint surfaces corresponding to individual platform legs in the kinematic mapping image space are classified and parametrized. The parametric equations are free from representational singularities. The entire set consists of hyperboloids of one sheet and hyperbolic paraboloids. This result corrects an oversight in the body of literature. These surfaces have important applications to the kinematic analysis of planar three-legged robot platforms, hence appropriate attention should be given to their classification.

Keywords: Kinematic mapping; Constraint surface; Planar parallel robot platform; Hyperboloid of one sheet; Hyperbolic paraboloid

1. Introduction

A very useful and elegant approach to the kinematic analysis of parallel robot platforms is *kinematic mapping*. A brief sampling of the literature justifies this statement, for example [1–8]. In this paper we use kinematic mapping to investigate the nature of the kinematic constraints of general three-legged planar platforms with three degrees of freedom (DOF). The only restriction on the architecture is that the joints all be lower pairs and that each of the three kinematic chains

* Corresponding author.
E-mail address: jhayes@mae.carleton.ca (M.J.D. Hayes).

0094-114X/03/$ - see front matter
doi:10.1016/S0094-114X(02)00128-3

connecting the platform to the fixed base be connected with three single DOF joints. The joints may be any combination of lower pairs. Each of the three sub-chains contains an actuated joint, although the active joints may be different in each leg. Platforms possessing holonomic higher pairs have been treated separately in [9–11].

In this paper we use a mapping of planar displacements that was introduced in 1911 simultaneously, and independently, by Grünwald [12] and Blaschke [13]. A very detailed account may be found in Bottema and Roth [14]. A natural question arises when constrained motions are considered: what form does the corresponding set of image points take? The answer, in principal, is simple: it depends on how the motion is constrained.

For general planar three-legged platforms (GP3LP) with three DOF we consider the motions of the platform by examining the motions of each leg separately. When the joints are restricted to lower pairs, *prismatic* (*P*) and *revolute* (*R*) pairs, then depending on the details of how the kinematic chain is arranged the image space point sets can be one of only two types: (1) if the constraint is linear (a point on the moving platform remains on a fixed line) the corresponding image space point set is an hyperbolic paraboloid; (2) if the constraint is circular (a point on the moving platform remains on a fixed circle) the corresponding image space point set is an hyperboloid of one sheet. Because these quadric surfaces contain the images of the constrained displacements, it is natural to call them *constraint surfaces*. Kinematic analysis of GP3LP reduces to intersection problems between the constraint surfaces for each leg.

The motivation for this work lies in the fact that the hyperbolic paraboloid has never been so identified. It has been, until now, classified as a *special hyperboloid* [3,14]. Because of their useful applications to platform forward and inverse kinematics [9,15,16], as well as workspace analysis [6,11,17], it is important to correctly classify the constraint surfaces.

2. Classifying general planar three-legged platforms

A GP3LP with three DOF consists of a moving platform connected to a fixed base by three simple kinematic chains. Each chain is connected by three independent one DOF joints, one of which is active. Thus each chain provides the control of one of three DOF of the moving platform. In this paper we will deal only with lower kinematic pair joints. Since the displacements of the platform are confined to the plane, only *R*- and *P*-pairs are considered.

The possible combinations of *R*- and *P*-pairs which connect the moving platform to the fixed base and constrain the independent open kinematic chains, consisting of successions of three joints starting from the fixed base, in a GP3LP are [18]:

$$RRR, RPR, RRP, RPP, PRR, PPR, PRP, PPP.$$

The *PPP* chain must be excluded because no combination of pure planar translations can cause a change in orientation. Thus, there are seven possible kinematic chains. Fig. 1 illustrates topologically symmetric platforms, each characterized by one of the seven allowable simple kinematic chains.

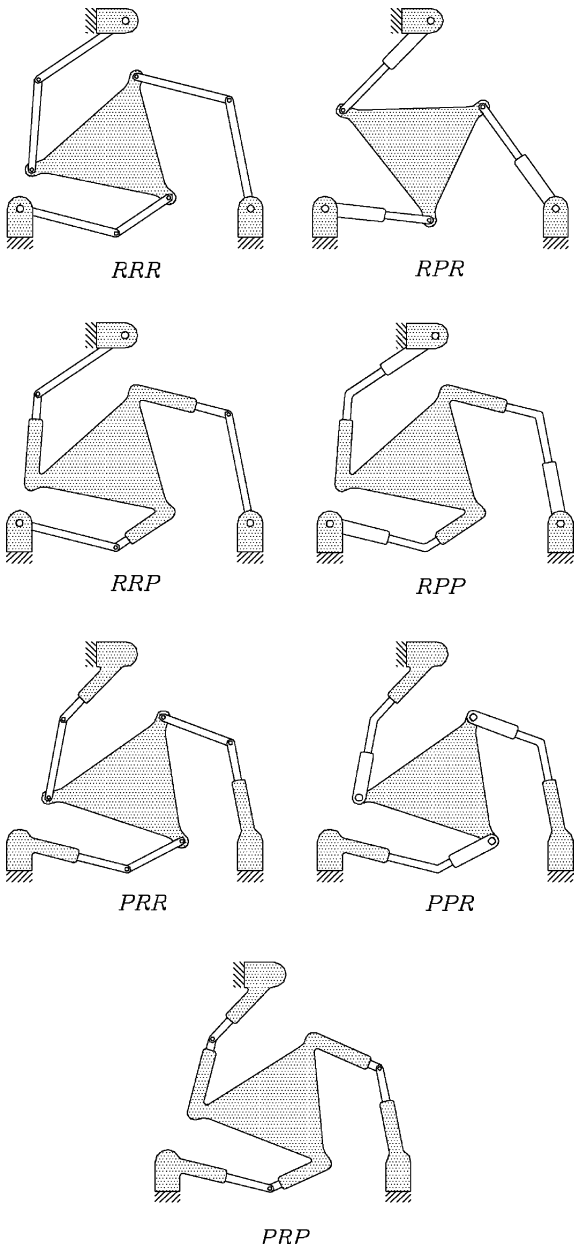

Fig. 1. The seven possible leg topologies in symmetric platforms.

2.1. Passive sub-chains

The active joint in a leg is identified with an underscore, *RPR*, for example. Since any one of the three joints in any of the seven allowable simple kinematic chains may be actuated there are twenty-one possible leg architectures.

Table 1
The 18 possible leg architectures

RR-type	*PR*-type	*RP*-type
$\underline{R}RR$	$\underline{R}PR$	$\underline{R}RP$
$R\underline{R}R$	$P\underline{R}R$	$R\underline{R}P$
$RR\underline{R}$	$PR\underline{R}$	$RP\underline{R}$
$\underline{P}RR$	$\underline{P}PR$	$\underline{P}RP$
$R\underline{P}R$	$P\underline{P}R$	$R\underline{P}P$
$RR\underline{P}$	$PR\underline{P}$	$RP\underline{P}$

When the value of the activated joint coordinate in a leg is specified, the joint is effectively locked and may be temporarily removed from the chain. What remains is a kinematic chain connected with two passive joints. Examining Fig. 1, it is to be seen that the resulting passive sub-chain is one of only four types: either *RR*, *PR*, *RP*, or *PP*. However, symmetric *PP*-type architecture must be rejected as not useful because such a platform either moves uncontrollably or is not assemblable when the actuated joint variables are specified [18,19]. Removing *PP*-type legs from the group reduces the number of possible leg architectures to eighteen. They are listed, according to passive sub-chain, in Table 1.

2.2. Enumerating the GP3LP

How many distinct GP3LP with three DOF are there? This number is arrived at by considering that there are 18 possible kinematic chains to choose from for each of three legs. If the elements are allowed to be counted more than once the number of possible combinations is given by

$$C(n,r) = \frac{(n+r-1)!}{r!(n-1)!} \Rightarrow C(18,3) = 1140. \tag{1}$$

3. The Grünwald–Blaschke mapping of plane kinematics

A general displacement in the plane requires three independent parameters to fully characterize it. The idea is to map the three independent quantities to the points of a 3-D projective image space. Referring to Fig. 2, the position of a point in a moving plane described by reference coordinate system E relative to a fixed plane described by coordinate system Σ can be given by the homogeneous linear transformation

$$\begin{bmatrix} X \\ Y \\ Z \end{bmatrix} = \begin{bmatrix} \cos\varphi & -\sin\varphi & a \\ \sin\varphi & \cos\varphi & b \\ 0 & 0 & 1 \end{bmatrix} \begin{bmatrix} x \\ y \\ z \end{bmatrix}, \tag{2}$$

where the ratios $(x : y : z)$ represent the homogeneous coordinates of a point in E, $(X : Y : Z)$ are those of the same point in Σ. The Cartesian coordinates of the origin of E measured in Σ are (a, b), while φ is the rotation angle measured from the X-axis to the x-axis, the positive sense being counter-clockwise. Clearly, in Eq. (2) the three characteristic displacement parameters are

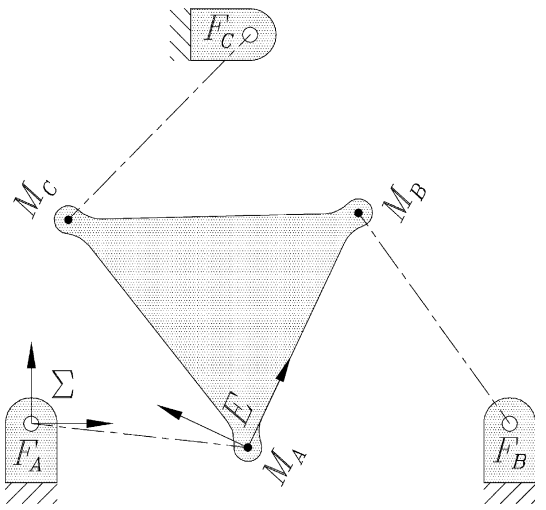

Fig. 2. The moving frame E and fixed frame Σ for any set of legs from Table 1.

(a, b, φ). Image points (points in the 3-D projective image space) are defined in terms of the displacement parameters (a, b, φ) as

$$(X_1 : X_2 : X_3 : X_4) = a\sin(\varphi/2) - b\cos(\varphi/2) : (a\cos(\varphi/2) + b\sin(\varphi/2) : 2\sin(\varphi/2) : 2\cos(\varphi/2)). \tag{3}$$

By virtue of the relationships expressed in Eq. (3), the transformation matrix from Eq. (2) may be expressed in terms of the homogeneous coordinates of the image space. This yields a linear transformation to express a displacement of E with respect to Σ in terms of the image point:

$$\begin{bmatrix} X \\ Y \\ Z \end{bmatrix} = \begin{bmatrix} (X_4^2 - X_3^2) & -2X_3X_4 & 2(X_1X_3 + X_2X_4) \\ 2X_3X_4 & (X_4^2 - X_3^2) & 2(X_2X_3 - X_1X_4) \\ 0 & 0 & (X_4^2 + X_3^2) \end{bmatrix} \begin{bmatrix} x \\ y \\ z \end{bmatrix}. \tag{4}$$

Since each distinct displacement described by (a, b, φ) has a corresponding unique image point, the inverse mapping can be obtained from Eq. (3): for a given point of the image space, the displacement parameters are

$$\begin{aligned} \tan(\varphi/2) &= X_3/X_4, \\ a &= 2(X_1X_3 + X_2X_4)/(X_3^2 + X_4^2), \\ b &= 2(X_2X_3 - X_1X_4)/(X_3^2 + X_4^2). \end{aligned} \tag{5}$$

Eq. (5) give correct results when either X_3 or X_4 is zero. Caution is in order, however, because the mapping is injective, not bijective: *there is at most one pre-image for each image point*. It is easy to see that any image point on the real line $X_3 = X_4 = 0$ has no pre-image and therefore does not correspond to a real displacement of E. The image point must satisfy the condition $X_3^2 + X_4^2 \neq 0$ in order to represent a real displacement. For a detailed discussion of singular cases see [14].

4. Kinematic constraints

Consider an arbitrary *RR*-type passive sub-chain. The leg architecture can be any of the six listed in the first column of Table 1. When the active joint variable in this leg is specified the sub-chain that remains has two passive *R*-pairs. Regardless of the leg architecture, once the active joint is locked one of the remaining *R*-pairs is fixed in Σ and the other moves on a circle of fixed radius centred on the stationary *R*-pair. Thus, the motions of an *RR*-type passive sub-chain are constrained by the fact that a point with fixed position in *E* moves on the circumference of a constant-radius, fixed-centred circle in Σ.

Next, consider an arbitrary *PR*-type passive sub-chain. These are listed in the second column of Table 1. When the active joint is locked the passive *R*-pair is constrained to move on a fixed line in Σ.

Finally, consider an arbitrary *RP*-type passive sub-chain, see the third column of Table 1. When the active joint is locked the passive *P*-pair is constrained to move on a fixed point in Σ. The kinematic constraint is represented by a planar pencil of lines on a point. When considered projectively, this constraint is nothing but the *dual* of the constraint for *PR*-type legs: a planar pencil of points on a line. Moreover, if *E* is considered as the fixed and Σ as the moving frame, the kinematic constraints for *RP*-type legs are identical to those of *PR*- and *RR*-type. In this sense *RP*-type legs can be considered as kinematic inversions of corresponding *PR*-type legs. Hence, the displacements of all *PR*- and *RP*-type passive sub-chain are governed by projectively identical kinematic constraints.

4.1. Circular constraints

The ungrounded *R*-pair in an *RR*-type leg is constrained to move on a circle with a fixed centre. Meanwhile, the platform can rotate about the moving *R*-pair. This two parameter family of displacements corresponds to a two parameter family of image points: a hyper-surface [14]. Its expression can be obtained in the following way: consider the motion of a fixed point in *E* that is constrained to move on a fixed circle in Σ, with radius *r*, centred on the homogeneous coordinates $(X_c : Y_c : Z)$ and having the equation

$$k_0(X^2 + Y^2) - 2XX_cZ - 2YY_cZ + X_c^2Z^2 + Y_c^2Z^2 - r^2Z^2 = 0. \tag{6}$$

Eq. (6) represents a circle only when $k_0 = 1$. However, to develop the constraint equations we shall leave it an arbitrary constant for the time being. It is convenient to express Eq. (6) in the following form:

$$k_0(X^2 + Y^2) + 2k_1XZ + 2k_2YZ + k_3Z^2 = 0, \tag{7}$$

where

$k_0 =$ arbitrary homogenising constant,
$k_1 = -X_c$,
$k_2 = -Y_c$,
$k_3 = k_1^2 + k_2^2 - r^2$.

Eq. (7) is homogeneously quadratic in the *variables* X, Y, Z, and homogeneously linear in the *constants* k_i, $i \in \{0,1,2,3\}$. There is then a dual relationship between the constants and the variables, in that Eq. (7) could represent the locus of variable points $(X : Y : Z)$ on a fixed circle with *circle coordinates* $[k_0 : k_1 : k_2 : k_3]$, or dually as a family of variable circles on a fixed point with point coordinates $(X : Y : Z)$. Thus, the four k_i, $i \in \{0,1,2,3\}$ are defined to be homogeneous circle coordinates, while X, Y, Z are the homogeneous *point coordinates* of the circle's point locus.

4.2. Linear constraints

If $k_0 = 0$ then Eq. (7) becomes

$$Z(2k_1X + 2k_2Y + k_3Z) = 0. \tag{8}$$

Eq. (8) represents two lines. The factor $Z = 0$ represents the line at infinity in the projective plane, P_2, while the factor in parentheses is the equation of a line where the first two *line coordinates* are multiplied by 2. The 2 can be treated as a proportionality factor arising from the original circle formulation of the equation of constraint. The *trivial* factor $Z = 0$ can be ignored because only ordinary lines (non-ideal lines) need be considered for practical designs. Looking at Eq. (8) it is to be seen that

$$[k_1 : k_2 : k_3] = \left[\frac{1}{2}L_1 : \frac{1}{2}L_2 : L_3\right], \tag{9}$$

where the L_i are line coordinates obtained by Grassmann expansion of the determinant of two points on the line [20].

An $\underline{R}PR$ leg will be used for illustration. For these legs the line coordinates are determined by the base R-pair inputs and the corresponding fixed point, F_i, $i \in \{A,B,C\}$ (see Fig. 2). The direction of the line is given by the base R-pair input: the joint angle with respect to the fixed base frame Σ, ϑ_Σ. Additionally, the location of a point on the line is known: the fixed revolute centre, also expressed in Σ, F_Σ. The line equation in Σ for a given leg is obtained from the Grassmann expansion:

$$\begin{vmatrix} X & Y & Z \\ F_{X/\Sigma} & F_{Y/\Sigma} & F_{Z/\Sigma} \\ \cos\vartheta_\Sigma & \sin\vartheta_\Sigma & 0 \end{vmatrix} = 0, \tag{10}$$

where the notation $F_{X/\Sigma}$, $F_{Y/\Sigma}$, $F_{Z/\Sigma}$, represent the homogeneous coordinates $(X : Y : Z)$ of the revolute centre relative to Σ. Applying Eq. (9) we obtain

$$[k_1 : k_2 : k_3] = \left[-\frac{F_{Z/\Sigma}}{2}\sin\vartheta_\Sigma : \frac{F_{Z/\Sigma}}{2}\cos\vartheta_\Sigma : (F_{X/\Sigma}\sin\vartheta_\Sigma - F_{Y/\Sigma}\cos\vartheta_\Sigma)\right]. \tag{11}$$

4.3. Image space constraint surface equations

The linear transformation in Eq. (4) gives the coordinates of points in the fixed frame Σ in terms of the points in the moving frame E and the kinematic mapping image points corresponding to a

particular displacement. An algebraic expression of the image space surface corresponding to the circular constraints emerges when the expressions for $(X : Y : Z)$ from Eq. (4) are substituted into Eq. (7):

$$\begin{aligned}&\Bigg(k_0z^2(X_1^2+X_2^2)+\frac{1}{4}\left[k_0(x^2+y^2)+k_3z^2-2z(k_1x+k_2y)\right]X_3^2\\&\quad+\frac{1}{4}\left[k_0(x^2+y^2)+k_3z^2+2z(k_1x+k_2y)\right]X_4^2+(k_1z^2-k_0xz)X_1X_3\\&\quad-(k_2z^2+k_0yz)X_1X_4+(k_2z^2-k_0yz)X_2X_3+(k_0xz+k_1z^2)X_2X_4\\&\quad+(k_2xz-k_1yz)X_3X_4\Bigg)\left(\frac{1}{4}(X_3^2+X_4^2)\right)=0.\end{aligned}\tag{12}$$

This quartic contains two quadratic factors in X_i. The factor $1/4(X_3^2+X_4^2)$ is exactly the non-zero condition of the planar kinematic mapping, which must be satisfied for a point to be the image of a real displacement. Since only the images of real displacements are considered, this factor must be non-zero and may be safely eliminated. What remains is a quadratic in the X_i. The quantities x, y, z (coordinates of leg-platform attachment points which have fixed position in E) and k_i are all design constants. Hence, the first factor in Eq. (12) is the point equation of a quadric surface in the 3-D projective image space. This general quadric is the geometric image of the kinematic constraint that a point in E moves on either a circle, or a line, in Σ depending on whether $k_0 = 1$, or $k_0 = 0$, respectively.

4.4. Identifying the quadric constraint surface

The first factor in Eq. (12) is greatly simplified under the following assumptions:

(1) No platform of practical significance will have a point at infinity, so it is safe to set $z = 1$.
(2) Platform rotations of $\phi = \pi$ (half-turns) have images in the plane $X_4 = 0$. Because the X_i are implicitly defined by Eq. (3), setting $\phi = \pi$ gives

$$(X_1 : X_2 : X_3 : X_4) = (a : b : 2 : 0).\tag{13}$$

When we remove the one parameter family of image points for platform orientations of $\phi = \pi$ we can, for convenience, normalise the image space coordinates by setting $X_4 = 1$.

Applying these assumptions to the first factor in Eq. (12) gives the simplified constraint surface equation:

$$\begin{aligned}&k_0(X_1^2+X_2^2)+\frac{1}{4}(k_0[x^2+y^2]+k_3-2[k_1x+k_2y])X_3^2+(k_1-k_0x)X_1X_3\\&\quad+(k_2-k_0y)X_2X_3-(k_2+k_0y)X_1+(k_0x+k_1)X_2+(k_2x-k_1y)X_3\\&\quad+\frac{1}{4}(k_0[x^2+y^2]+k_3+2[k_1x+k_2y])=0.\end{aligned}\tag{14}$$

The constraint surface can be identified in many ways. We proceed in an intuitive way by employing some careful geometric thinking. There are two cases to consider: (1) if the leg is *RR*-

type, the k_i are circle coordinates and one must set $k_0 = 1$; and (2) if the leg is *PR*- or *RP*-type, the k_i are proportional to line coordinates and it is necessary to set $k_0 = 0$.

4.5. RR-type: hyperboloid of one sheet

Setting $k_0 = 1$ in Eq. (14) gives the following:

$$\begin{aligned} H : {} & X_1^2 + X_2^2 + \frac{1}{4}(x^2 + y^2 + k_3 - 2[k_1 x + k_2 y])X_3^2 + (k_1 - x)X_1 X_3 \\ & + (k_2 - y)X_2 X_3 - (k_2 + y)X_1 + (x + k_1)X_2 + (k_2 x - k_1 y)X_3 \\ & + \frac{1}{4}(x^2 + y^2 + k_3 + 2[k_1 x + k_2 y]) = 0. \end{aligned} \tag{15}$$

This surface is seen to be an hyperboloid of one sheet, hence indicated by H, after the subsequent arguments are considered. Intersections of the quadric with planes where $X_3 =$ constant are studied. First we rewrite $k_3 = k_1^2 + k_2^2 - r^2$ in Eq. (15) (recall r is the radius of the circle centred at $(-k_1, -k_2)$. Collect X_1 and X_2 terms on the left and constant terms, including X_3 terms, on the right-hand side of the equation, then complete the squares in X_1 and X_2. After some algebra the following equation is obtained:

$$\left(X_1 - \frac{1}{2}[\{x - k_1\}X_3 + k_2 + y]\right)^2 + \left(X_2 - \frac{1}{2}[\{y - k_2\}X_3 - k_1 - x]\right)^2 = \frac{r^2}{4}(1 + X_3^2). \tag{16}$$

Eq. (16) represents a circle in the planes where X_3 is a constant. The circle centre has coordinates

$$\left(\frac{1}{2}[\{x - k_1\}X_3 + k_2 + y] : \frac{1}{2}[\{y - k_2\}X_3 - k_1 - x] : X_3\right), \tag{17}$$

and radius

$$R_{X_3} = \frac{r}{2}\sqrt{(1 + X_3^2)}. \tag{18}$$

As X_3 is varied, the locus of circle centres defines a line. Setting $X_3 = t$, the linear parametric equation is

$$\begin{bmatrix} X_1 \\ X_2 \\ X_3 \end{bmatrix} = \frac{1}{2}\begin{bmatrix} k_2 + y \\ -k_1 - x \\ 0 \end{bmatrix} + \frac{t}{2}\begin{bmatrix} x - k_1 \\ y - k_2 \\ 2 \end{bmatrix}. \tag{19}$$

This leads to the conclusion that the quadric surface is a family of generally non-concentric circles whose centre points are all collinear. Furthermore, it is apparent from Eq. (16) that the smallest circle of the family occurs when $X_3 = 0$, and has a radius equal to $r/2$. As X_3 increases in value the circles become larger regardless of the sign of X_3. Thus, the quadric surface extends to infinity in two directions.

It is well known that there are only nine different types of quadrics [21]. Intersections of certain planes with spheres and ellipsoids contain circles, but the surfaces are finite. Parabolic cylinders

extend to infinity in only one direction, moreover no real plane intersections contain circles. The hyperbolic cylinders extend to infinity in two directions, but, like the parabolic cylinders, no real plane intersections contain circles. Circular cylinder plane intersections contain circles, but all of the same diameter. Additionally, cones contain circles, but contain a degenerate one with vanishing diameter. Every plane intersects an hyperbolic paraboloid in either a parabola, an hyperbola, or two lines; no circles. It cannot be an hyperboloid of two sheets because it is a continuous family of circles, the smallest radius being finite. Hence, by process of elimination, the only possible quadric surface that fits the geometric description of the constraint surface is an hyperboloid of one sheet.

The locus of circle centres, $\mathscr{L}$, is given by Eq. (19). Note that $\mathscr{L}$ is not necessarily perpendicular to the circles. The line $\mathscr{L}$ is unique and planes to which it is orthogonal, in general, intersect the hyperboloid in ellipses. Thus, the hyperboloid is generally not one of revolution, it is skew. However, the hyperboloid always intersects the planes parallel to $X_3 = \text{constant}$ in circles. Thus, the X_3-axis is perpendicular to the circles. If, however, $k_1 = k_2 = x = y = 0$ then $\mathscr{L}$ and the longitudinal axis of the hyperboloid coincide with the X_3-axis.

4.6. Parametric equation of the constraint hyperboloid

If computer generated images of the constraint hyperboloid are required then a parametrization is necessary. The parametric equation of a second order surface requires two parameters. The implicit form of the constraint hyperboloid, Eq. (15), represents a circle in the projection of the intersection of the two hyper-planes $X_3 = \text{constant}$ and $X_4 = 1$. An arbitrary hyperboloid circle can be parametrized with an angle ζ. The radius of the circle can then be changed by varying the parameter t, see Fig. 3. The hyperboloid circle equation may be written as

$$(X_1 - X_{1c})^2 + (X_2 - X_{2c})^2 - R_{X_3}^2 = 0, \tag{20}$$

where (X_{1c}, X_{2c}) are the coordinates of the circle centre and R_{X_3} is its radius.

The locus of points satisfying Eq. (20) can be generated parametrically with the angle ζ such that the following vector equation is fulfilled:

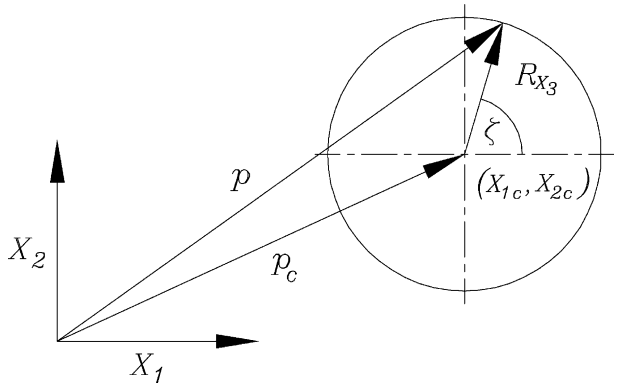

Fig. 3. An arbitrary hyperboloid circle.

$$\boldsymbol{p} = \boldsymbol{p}_c + \boldsymbol{R}_{X_3}(\zeta). \tag{21}$$

Using the expressions in Eq. (16) with $X_3 = t$, Eq. (21) can be rewritten in component form, giving the parametric form of the constraint hyperboloid in terms of the two parameters t and ζ:

$$\begin{bmatrix} X_1 \\ X_2 \\ X_3 \end{bmatrix} = \frac{1}{2}\begin{bmatrix} ([x-k_1]t + k_2 + y) + (r\sqrt{t^2+1})\cos\zeta \\ ([y-k_2]t - k_1 - x) + (r\sqrt{t^2+1})\sin\zeta \\ 2t \end{bmatrix},$$
$$\zeta \in \{0,\ldots,2\pi\},\quad t \in \{-\infty,\ldots,\infty\}. \tag{22}$$

Fig. 4 is a parametric representation of a constraint hyperboloid with $k_1 = -1$, $k_2 = -3$, $r = 2$, and the moving platform points have coordinates $x = 1$, $y = 3$.

4.7. PR- and RP-type: hyperbolic paraboloid

A very different constraint surface is obtained when the displacement condition is changed so that a fixed point in the moving frame E is constrained to move on a fixed line in the non-moving frame Σ. This condition requires the k_i to represent planar line coordinates. Hence, it is necessary to set $k_0 = 0$ in Eq. (14). Making this substitution we obtain an hyperbolic paraboloid, indicated by HP:

$$\mathrm{HP}: (k_1X_3 - k_2)X_1 + (k_1 + k_2X_3)X_2 + \frac{1}{4}(k_3 - 2[k_1x + k_2y])X_3^2$$
$$+ (k_2x - k_1y)X_3 + \frac{1}{4}(k_3 + 2[k_1x + k_2y]) = 0. \tag{23}$$

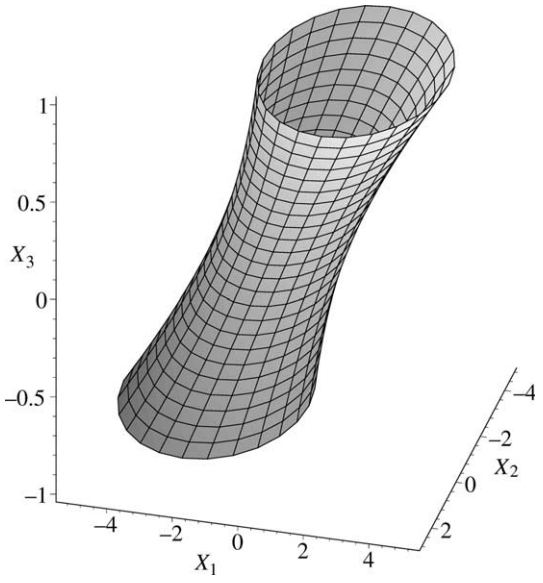

Fig. 4. A projection of H in the hyper-plane $X_4 = 1$.

This is seen to be true after the following argument is considered. Eq. (23) is a quadric in the X_i, but very different in form from Eq. (15). To compare them, Eq. (23) is also intersected with planes where X_3 is a constant. As X_3 is varied a family of mutually skew lines is obtained that are all parallel to a plane, but not to each other. The quadric is therefore a regulus of an hyperbolic paraboloid [21]. This being the case, it cannot be classified as a special hyperboloid as in [3] and [14].

4.8. Parametric equation of the constraint hyperbolic paraboloid

There is usually more than one way to parametrize a surface. We propose the following one because it is free from representational singularities. That is, some of the components of the parametric equation may consist of fractions. The denominators must be free from dependence on the parameters. One way to achieve this is to use the proposed directrix.

The hyperbolic paraboloid can be constructed using a line, $\mathscr{L}$, in one regulus, $\mathscr{R}$, as the directrix for the opposite regulus, $\mathscr{R}_0$. This can be done because for all doubly ruled quadric surfaces each line in regulus $\mathscr{R}$ intersects every line in the opposite regulus, $\mathscr{R}_0$.

When $X_3 = 0$ then Eq. (23) represents the line $\mathscr{L}_0$ contained in the plane $X_3 = 0$, indicated by $\pi_{X_3} = 0$. Now, consider the plane π that also contains $\mathscr{L}_0$, but is perpendicular to $\pi_{X_3} = 0$, see Fig. 5. The X_3-axis is parallel to π. Let the line $\mathscr{L}_0$ be one line in regulus $\mathscr{R}_0$. There is one and only one line $\mathscr{L}$ contained in the intersection of regulus $\mathscr{R}$ and plane π. Since $\mathscr{L}$ intersects every line in $\mathscr{R}_0$, every distinct point on $\mathscr{L}$ represents an intersection with a distinct line in $\mathscr{R}_0$. The locus of points on $\mathscr{L}$ is a function of the parameter $X_3 = t$.

A general line in space can be described by a fixed point on the line along with a direction. For every value of t there is a unique point on the directrix line $\mathscr{L}$, which is the point of intersection with the corresponding line $\mathscr{L}_i \in \mathscr{R}_0$. The direction of $\mathscr{L}_i$ is also a function of t since this line must be parallel to $\pi_{X_3} = t$. Stepping in the direction of $\mathscr{L}_i$ by varying a second parameter s yields the locus of points on $\mathscr{L}_i$:

$$\mathscr{L}_i = \mathrm{HP} = \begin{bmatrix} f(t) \\ g(t) \\ t \end{bmatrix} + s \begin{bmatrix} a(t) \\ b(t) \\ 0 \end{bmatrix}. \tag{24}$$

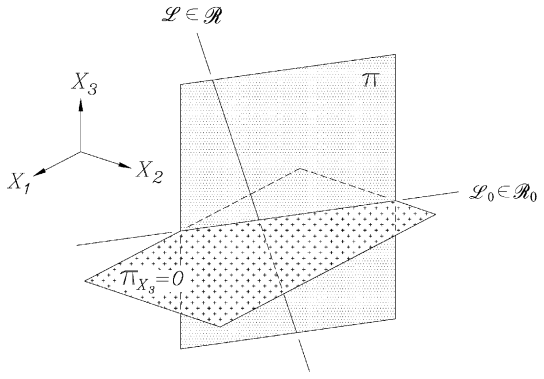

Fig. 5. Constructing an hyperbolic paraboloid.

This collection of lines is a quadric by virtue of the mixed second order quantities $sa(t)$ and $sb(t)$. Determining the functions $f(t)$, $g(t)$, $a(t)$ and $b(t)$ will yield the parametrization of the constraint HP.

The first step is to determine the plane π that is perpendicular to the plane $\pi_{X_3} = 0$. The equation for $\mathscr{L}_0$ is obtained after setting $X_3 = 0$ in Eq. (23):

$$\mathscr{L}_0 : -k_2X_1 + k_1X_2 + \frac{1}{4}(k_3 + 2[k_1x + k_2y]) = 0. \tag{25}$$

The line $\mathscr{L}_0$ is the line of intersection of the two planes $\pi_{X_3} = 0$ and π. The plane π is perpendicular to $\pi_{X_3} = 0$ and must also contain $\mathscr{L}_0$. Due to this, π can be described by solving Eq. (25) for either X_1 or X_2 and allowing X_3 to take on any value. Solving for X_1 we obtain

$$\pi = \begin{cases} X_1 = \frac{1}{k_2}\left(k_1X_2 + \frac{1}{4}[k_3 + 2\{k_1x + k_2y\}]\right), \\ X_3 = X_3. \end{cases} \tag{26}$$

If k_2 is close to zero, then Eq. (25) is solved for X_2, giving

$$\pi = \begin{cases} X_2 = \frac{1}{k_1}\left(-k_2X_1 + \frac{1}{4}[k_3 + 2\{k_1x + k_2y\}]\right), \\ X_3 = X_3. \end{cases} \tag{27}$$

Note that k_1 and k_2 cannot simultaneously vanish because they are proportional to line coordinates of the real line between corresponding pairs of fixed base points and moving platform leg attachment points. Either representation of the plane π, Eq. (26) or Eq. (27), may be used yielding identical results.

Without loss in generality k_2 can be assumed sufficiently large for this derivation. Eq. (26) mean that any point $[X_1 : X_2 : X_3] \in \pi$ is given by choosing values for X_2 and X_3. Thus, the plane π, which is perpendicular to $\pi_{X_3} = 0$, is completely described by the first of Eq. (26), since X_2 and X_3 are arbitrary, and independent.

The next step is to find an expression for $\mathscr{L} \in \mathscr{R}$. This is done by finding the line of intersection of π and the implicit equation of the hyperbolic paraboloid, Eq. (23). This is the unique line in $\mathscr{R}$ contained in π which intersects $\mathscr{L}_0 \in \mathscr{R}_0$. This equation is obtained by substituting the first of Eq. (26) into Eq. (23), yielding

$$\frac{X_3}{4k_2}\left(4[k_1^2 + k_2^2]X_2 + [k_2k_3 - 2\{k_2^2y + k_1k_2x\}]X_3 + 2[k_1^2 + 2k_2^2]x - 2k_1k_2y + k_1k_3\right) = 0, \tag{28}$$

assuming k_2 is sufficiently large. This intersection apparently contains two factors, the plane $X_3 = 0$, and the line

$$\mathscr{L} : 4(k_1^2 + k_2^2)X_2 + \left(k_2k_3 - 2[k_2^2y + k_1k_2x]\right)X_3 + 2(k_1^2 + 2k_2^2)x + k_1k_3 = 0. \tag{29}$$

This does not agree with the fact that a plane intersecting with a quadric must produce a second order curve. Here the conic should degenerate into two lines. In fact, it does. The first factor is an artifact of the representation. Recall Fig. 5 and Eq. (25), the plane $X_3 = 0$ contains the line $\mathscr{L}_0$ and no other line of the quadric. Then Eq. (29) *must* be an expression for $\mathscr{L}$, since it is a line contained in the intersection of π and HP that is *not* $\mathscr{L}_0$. Since $\mathscr{L}_0$ and $\mathscr{L}$ intersect, and because they are both in HP, these lines are in the opposite reguli $\mathscr{R}_0$ and $\mathscr{R}$.

Now, solve Eq. (29) for X_2. After setting $X_3 = t$ the following expression is obtained:

$$g(t) = \frac{(2[k_1k_2x + k_2^2y] - k_2k_3)t - 2(k_1^2 + 2k_2^2)x + 2k_1k_2y - k_1k_3}{4(k_1^2 + k_2^2)}, \tag{30}$$

which represents the X_2 coordinate of a point on the line $\mathscr{L} \in \mathscr{R}$ for a particular value of t. The X_1 coordinate is obtained by substituting the expression for $X_2 = g(t)$ into Eq. (26) which yields another function of only t:

$$f(t) = \frac{(2[k_1k_2y + k_1^2x] - k_1k_3)t + 2(2k_1^2 + k_2^2)y - 2k_1k_2x + k_2k_3}{4(k_1^2 + k_2^2)}. \tag{31}$$

This gives the desired parametric equation for $\mathscr{L}$ in terms of $X_3 = t$. Note that the denominators of the rational functions $f(t)$ and $g(t)$ are identical: $k_1^2 + k_2^2$. Moreover, the denominator is non-vanishing because k_1^2 and k_2^2 are, for the linear kinematic constraints, line coordinates and cannot simultaneously be zero.

Now, direction vectors for the $\mathscr{L}_i$ are required. The coefficients in Eq. (23) are constants, and may be collected giving

$$aX_1 + bX_2 + cX_3^2 + dX_3 + e = 0, \tag{32}$$

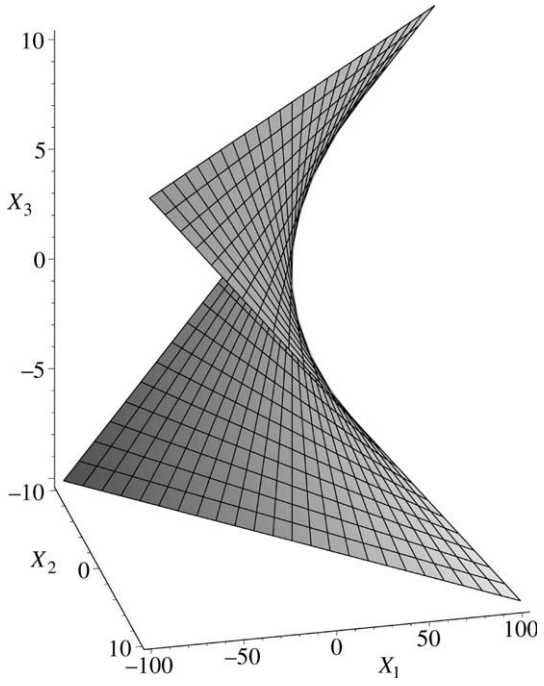

Fig. 6. A projection of HP in the hyper-plane $X_4 = 1$.

where a and b are both functions of $X_3 = t$. In an arbitrary plane $\pi_{X_3} = t$ the direction of the corresponding line is given by the coefficient ratio $-b/a$, i.e., the slope of the line in the given plane. In other words, the line $\mathscr{L}_i$ is parallel to the direction given by

$$a(t)X_1 + b(t)X_2 = 0, \tag{33}$$

where

$$a(t) = k_1 t - k_2, \tag{34}$$

$$b(t) = k_1 + k_2 t. \tag{35}$$

Combining the points on the directrix with the directions of the lines in the regulus gives the desired parametrization of the constraint HP:

$$\mathrm{HP}: \begin{bmatrix} X_1 \\ X_2 \\ X_3 \end{bmatrix} = \begin{bmatrix} f(t) \\ g(t) \\ t \end{bmatrix} + s \begin{bmatrix} -b(t) \\ a(t) \\ 0 \end{bmatrix}, \quad -\infty \leqslant t \leqslant \infty, \quad -\infty \leqslant s \leqslant \infty. \tag{36}$$

Fig. 6 illustrates a parametric representation of a constraint hyperbolic paraboloid with circle coordinates $k_0 = 0$, $k_1 = 1$, $k_2 = k_3 = 0$, and fixed platform point coordinates $x = y = 0$.

5. Conclusions

In this paper we have shown that the only possible kinematic mapping image space surfaces corresponding to the kinematic constraints in arbitrary legs of a GP3LP are either hyperboloids of one sheet, or hyperbolic paraboloids. Our tools for classifying these constraint surfaces were elementary concepts of classical geometry regarding quadrics in three dimensional Cartesian space. Parametrizations for each constraint surface were derived. The parametrizations are always implementable because they are singularity free regarding the parameters. These surfaces are important in the applications to kinematic analysis of GP3LP: the forward and inverse kinematic problems [9,15,19], together with workspace analysis and visualization [6,11,17].

References

[1] S. De Sa, B. Roth, Kinematic mappings. Part 1: Classification of algebraic motions in the plane, ASME J. Mech. Des. 103 (1981) 585–591.
[2] S. De Sa, B. Roth, Kinematic mappings. Part 2: Rational algebraic motions in the plane, ASME J. Mech. Des. 103 (1981) 712–717.
[3] B. Ravani, B. Roth, Motion synthesis using kinematic mappings, ASME J. Mech. Transmissions Autom. Des. 105 (1983) 460–467.
[4] B. Ravani, B. Roth, Mappings of spatial kinematics, ASME J. Mech. Transmissions Autom. Des. 106 (1984) 341–347.
[5] M. Husty, An algorithm for solving the direct kinematics of general Stewart-Gough platforms, Mech. Mach. Theory 31 (4) (1996) 365–379.
[6] M. Husty, On the workspace of planar three-legged platforms, Proc. World Autom. Conf., 6th Int. Symposium on Rob. and Manuf. (ISRAM 1996), Montpellier, France, vol. 3, 1996, pp. 339–344.
[7] C. Collins, J. McCarthy, The quartic singularity surface of planar platforms in the Clifford algebra of the projective plane, Mech. Mach. Theory 33 (7) (1998) 931–944.

[8] A. Murray, F. Pierrot, N-position synthesis of parallel planar RPR platforms, in: J. Lenarčič, M.L. Husty (Eds.), Advances in Robot Kinematics: Analysis and Control, Kluwer Academic Publishers, Dordrecht, The Netherlands, 1998, pp. 69–78.
[9] M. Hayes, P. Zsombor-Murray, Inverse kinematics of a planar manipulator with holonomic higher pairs, in: J. Lenarčič, M.L. Husty (Eds.), Recent Advances in Robotic Kinematics, Kluwer Academic Publishers, Dordrecht, The Netherlands, 1998, pp. 59–68.
[10] M. Hayes, M. Husty, P. Zsombor-Murray, Solving the forward kinematics of a planar 3-legged platform with holonomic higher pairs, ASME J. Mech. Des. 121 (2) (1999) 212–219.
[11] M. Hayes, M. Husty, Workspace characterization of planar three-legged platforms with holonomic higher pairs, in: J. Lenarčič, Stanišić (Eds.), Advances in Robotic Kinematics, Kluwer Academic Publishers, Dordrecht, The Netherlands, 2000, pp. 267–276.
[12] J. Grünwald, Ein Abbildungsprinzip welches die ebene Geometrie und Kinematik mit der räumlichen Geometrie verknüpft, Sitzber. Ak. Wiss. Wien 120 (1911) 677–741.
[13] W. Blaschke, Euklidische Kinematik und Nichteuklidische Geometrie, Zeitschr. Math. Phys. 60 (1911) 61–91, pp. 203–204.
[14] O. Bottema, B. Roth, Theoretical Kinematics, Dover Publications Inc., New York, NY, USA, 1990.
[15] M. Husty, Kinematic mapping of planar three-legged platforms, Proc. 15th Canadian Congress of Applied Mechanics (CANCAM 1995), Victoria, BC, Canada, vol. 2, 1995 pp. 876–877.
[16] M. Hayes, M. Husty, P. Zsombor-Murray, Kinematic mapping of planar Stewart-Gough platforms, Proc. 17th Canadian Congress of Applied Mechanics (CANCAM 1999), Hamilton, Ont., Canada, 1999, pp. 319–320.
[17] M. Hayes, M. Husty, P. Zsombor-Murray, Towards workspace analysis of platforms with three arbitrary legs, Proc. 18th Canadian Congress of Applied Mechanics (CANCAM), St. John's, Nfld., Canada, 2001, pp. 355–356.
[18] J.-P. Merlet, Direct kinematics of planar parallel manipulators, IEEE Int. Conf. on Robotics and Automation, Minneapolis, USA, 1996, pp. 3744–3749.
[19] M. Hayes, Kinematics of general planar stewart-gough platforms, Ph.D. thesis, Department of Mechanical Engineering, McGill University, Montréal, Que., Canada, 1999.
[20] F. Klein, Elementary Mathematics from an Advanced Standpoint: Geometry, Dover Publications Inc., New York, NY, USA, 1939.
[21] D. Hilbert, S. Cohn-Vossen, Geometry and The Imagination, English translation by P. Nemenyi of Anschauliche Geometrie, 1932, Chelsea Publishing Company, New York, NY, USA, 1952.